Energy Transport in Radio Galaxies and Quasars
ASP Conference Series, Vol. 100, 1996
P. E. Hardee, A. H. Bridle, and J. A. Zensus (eds.)

The Jets in the Radio Galaxy 3C 353

MARK R. SWAIN[1] AND ALAN H. BRIDLE
National Radio Astronomy Observatory,
520 Edgemont Road, Charlottesville, VA 22903-2475, U.S.A.

STEFI A. BAUM
Space Telescope Science Institute,
3700 San Martin Drive, Baltimore, MD 21218, U.S.A.

Abstract. Well-sampled multi-configuration VLA images of the nearby FR II radio galaxy 3C 353 show both of its jets at exceptionally high transverse resolution—up to eight beamwidths across. The jets contribute ~1% of the integrated flux density at 5 GHz. Both are well-collimated. Their transverse intensity profiles are typically flat-topped, not center-brightened. The brighter jet is surrounded by a "sheath" of enhanced emission about three to five jet widths in extent, and roughly coaxial with it. The jets appear to be only weakly linearly polarized, but there are striking *minima* in both the polarized intensity and degree of polarization of the total emission along their edges. We interpret these minima to imply that the jet edges are dominated by a magnetic field configuration whose component in the plane of the sky is predominantly *parallel* to the jet axis, so that their polarized emission cancels that from surrounding regions (whose field is predominantly *perpendicular* to the jet axes).

1. Introduction

3C 353 is a V = 15.4 elliptical galaxy that is the dominant member of a Zwicky cluster at $z = 0.03$. It has a broad double-lobed radio structure with a well-defined hot spot in one lobe, making it clearly of Fanaroff-Riley Class II. For $H_0 = 100h$ km s^{-1} Mpc^{-1}, its projected linear size is $\sim 120h^{-1}$ kpc, and its radio luminosity is $5h^{-2} \times 10^{25}$ W Hz^{-1} at 1.4 GHz. It is thus slightly larger than, and has about one-hundredth the radio luminosity of, Cygnus A. 3C 353 has hitherto received little attention (for such a strong source—57 Jy at 1.4 GHz) because of its equatorial declination ($\delta = -0\overset{\circ}{.}9$) and low galactic latitude ($b = 19\overset{\circ}{.}6$). We have remedied this by making well-sampled (multi-configuration) VLA images of 3C 353 at 1.4, 1.7, 4.9 and 8.4 GHz. Figure 1 shows a composite (A+B+C+D-configuration) total intensity image with $0\overset{''}{.}44$ resolution at 8.4 GHz.

[1]also Department of Physics & Astronomy, University of Rochester, Rochester, NY 14627, U.S.A.

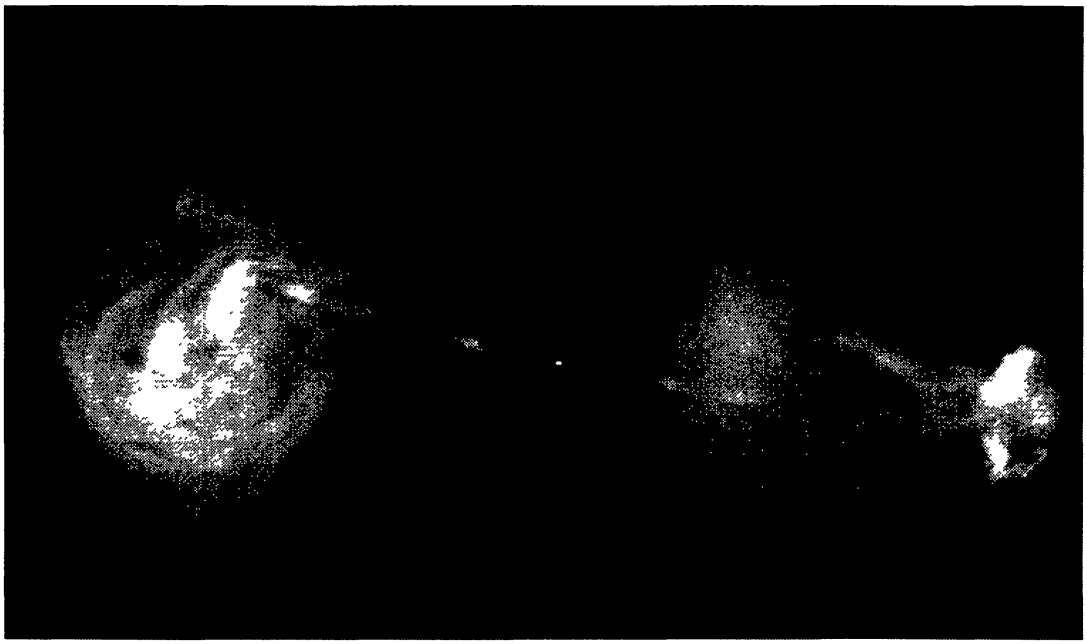

Figure 1. 3C 353 at 8.4 GHz with 0.″44 (FWHM) resolution.

2. Total Intensity Features

The following features of 3C 353 are evident from Figure 1:

1. The jet and counterjet, which comprise about 1% of the total emission from the source, are both well-collimated.

2. Both jets brighten significantly beyond $\sim 10h^{-1}$ kpc from the nucleus.

3. Both jets contain knots of enhanced brightness within more diffuse, roughly parallel-sided (i.e., slowly-expanding), emission.

4. Both lobes are highly filamentary. Filamentation in the West lobe confuses the outer path of the counterjet, so it is hard to identify which, if any, features in the outer lobe might continue the counterjet.

5. The integrated flux density of the jet is between two and three times that of the unambiguous segment of the counterjet.

6. The jet, which is relatively straight along p.a. 73.°8 for most of its length, can be traced all the way from its first bright knot to a well-defined, oblique hot spot that has a prominent arc of emission on its north rim.

7. In contrast, the counterjet first appears at p.a. $\sim 78.^{\circ}5$, then deflects to p.a. $\sim 85^{\circ}$ before reaching a complex ring of emission containing much substructure but no well-defined "hot spot".

8. Although the jet is straight, its centerline does not point to the nuclear source; its north edge aligns better with the nucleus.

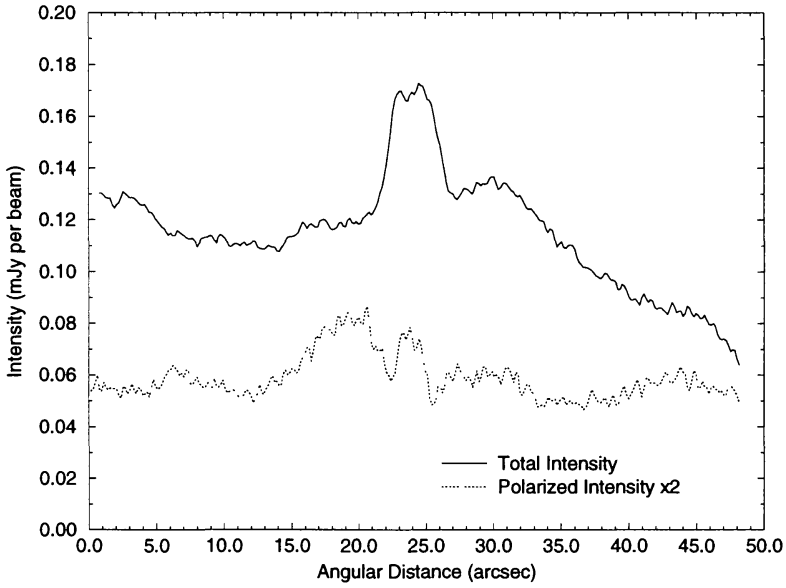

Figure 2. Averaged transverse profiles across the segment of the jet between the brightest knots: 8.4 GHz, 0.″44 (FWHM) resolution. *Upper:* total intensity. *Lower:* polarized intensity ×2, showing two minima.

3. Transverse Profiles Across the Jet

We have used transverse profiles of the total and polarized intensity across the jets to search for other features that may be coaxial with them (and which may therefore visualize related features of the outflow).

3.1. Total intensity

Flat-topped jet and counterjet profiles The transverse intensity profiles are flat-topped in many regions (see Figure 2, upper curve). The profiles are poorly fitted by single Gaussian components wherever the signal-to-noise is high. Residuals from Gaussian fits are always positive toward the edges of the jet, and negative toward the jet axis.

The "sheath" around the jet The total intensity profiles shown in Figures 2 and 3 illustrate that there is also excess emission within three to five jet radii (4 to 8 h^{-1} kpc) of the jet axis. This excess, or "sheath", is *not* simply a broad band around the jet that is fully filled with diffuse emission. As well as some diffuse emission, it contains bright ridges resembling the lobe filaments, and a relative absence of emission close to the jet.

The transverse-integrated intensity of the sheath tends to increase with that of the jet (Figure 4). The sheath is first detected at about the same distance from the nucleus as the first jet knot, but brightens less abruptly than the jet. Its ridge-like substructure complicates quantifying its collimation, or how well it aligns with the jet; but integrating transverse profiles of total and polarized intensity along axes at 0°, ±10° and ±20° to the jet implies that sheath and jet are coaxial to $\leq 10°$. We cannot exclude the possibility that the sheath is merely part of the filamentary structure of the lobe that is superposed on the jet by

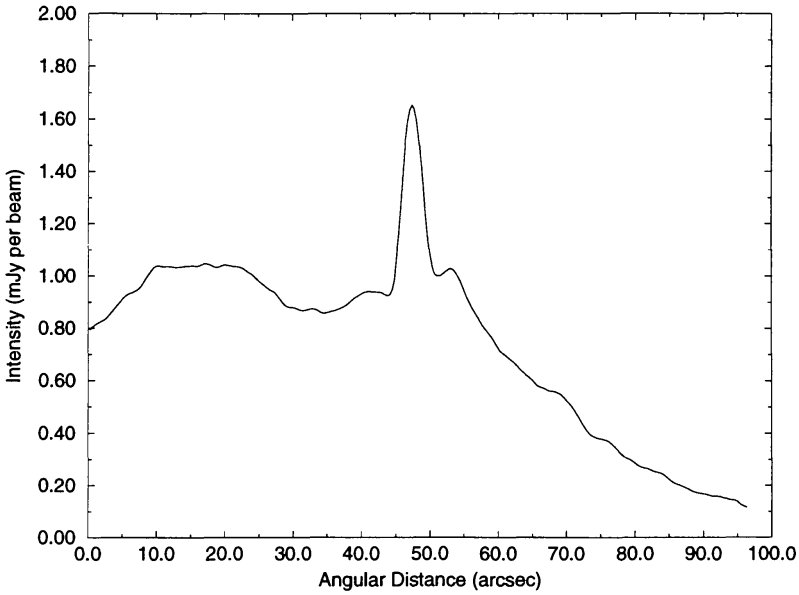

Figure 3. Averaged transverse intensity profile across the entire jet at 8.4 GHz with 1.″3 (FWHM) resolution.

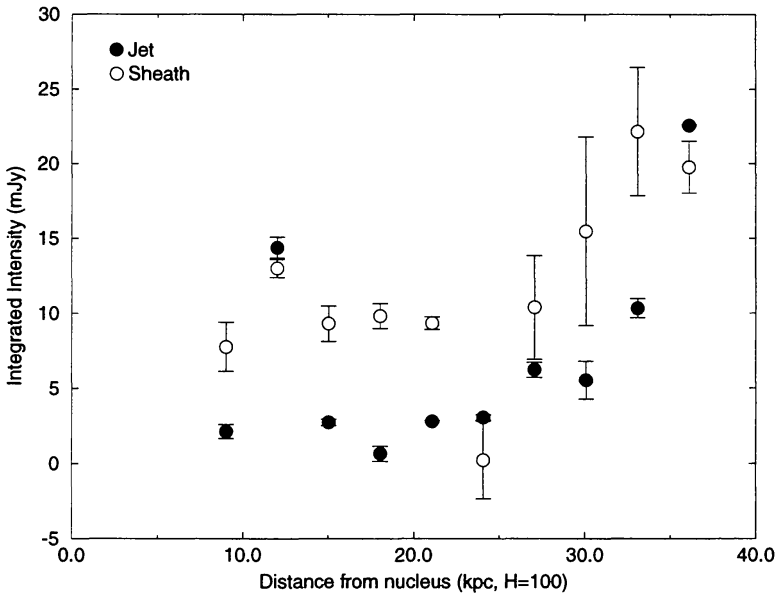

Figure 4. Transverse-integrated intensity of the jet and of the "sheath" plotted against distance from the nucleus.

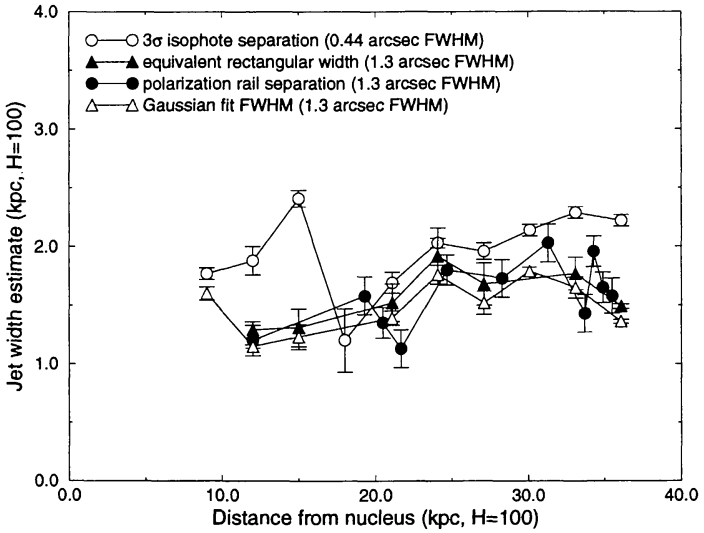

Figure 5. Four jet collimation measures, showing little spreading.

chance. The connection between their intensities (Figure 4) suggests, however, that the sheath includes features that influence, or are influenced by, the passage of the jet. There is no evidence of a similar sheath around the counterjet.

3.2. Polarized intensity—the "rails"

At all wavelengths, the polarized intensity and the degree of linear polarization have well-defined minima near both edges of both jets, but (away from the brightest knots) neither jet exhibits much excess polarization on-axis. These "rails" of depressed polarized intensity are near the half-power points of both jets, as illustrated for the main jet in Figure 2. The depth of the "rails" is typically from 20% to 40% of the total intensity of the jet at their locations, and they are not seen anywhere there is no jet emission.

We believe that these pairs of polarization "rails" indicate a systematic misalignment between the dominant magnetic field components near the edges of the jets and in surrounding (lobe plus sheath) emission. Four-frequency fits to the Faraday rotation measure over 3C 353 show that the apparent (synchrotron-emissivity weighted, line-of-sight averaged) magnetic field in the emission around both jets is predominantly, but not exclusively, *perpendicular* to the jet axes. The "rails" can therefore be accounted for by the crossed-field configuration that results if the apparent field near the edges of the jets is predominantly axial, while that near their centers is disordered, or is dominated by toroidal or radial components. *Such a configuration may occur if a velocity shear converts radial field components to axial field in the outer layers of a quasi-cylindrical jet.* We suggest that if 3C 353's jets could be studied in isolation, they would be limb-brightened in polarization, with the apparent magnetic field direction parallel to the jet axis towards both edges of both jets.

3.3. Collimation of the jet and counterjet

Figure 5 plots four measures of the width of the main jet against distance from the nucleus, wherever the uncertainty in the estimate is $< 0.5h^{-1}$ kpc. By all four

measures, including the separation of the polarization "rails", the jet expands only slowly, if at all, over most of its length. *Both* jets can be described as features that are roughly constant ($\sim 1.5h^{-1}$ kpc) in width, containing narrower bright knots which locally perturb the individual width measures.

4. Discussion and Conclusions

1. The counterjet is not a faint replica of the main jet, either in geometry or in brightness. We therefore see little reason to ascribe the primary jet/counterjet intensity asymmetry in 3C 353 to relativistic beaming.

2. The two jets terminate differently. The straighter jet forms a well-defined, oblique, hot spot. The counterjet bends, dims (and perhaps disrupts) entering a ring of emission around the jet axis with no clear hot spot.

3. There is enhanced emission on the scale of about five jet radii around, and approximately coaxial with, the obvious jet in 3C 353. A similar scale of excess emission was seen around the jet in the FR II radio galaxy 3C 219 by Clarke et al. (1992). This scale also resembles that of the "channel" around the counterjet in Cygnus A noted by Katz-Stone & Rudnick (1994). The dynamical significance of such emission "sheaths" around jets in FR II sources is unclear, but their existence questions whether the brightest jet-like synchrotron emission visualizes all components of the outflows.

4. There is good evidence for a region of enhanced polarization, with the apparent magnetic field along the jet direction, toward the outer edges of both jets in 3C 353. This feature resembles the shear layer on the outside of FR I jets in Laing's (1993, and these Proceedings, Page 241) decelerating-jet model. For a jet near the plane of the sky, this field structure, and some "Doppler hiding" of the emission near the jet axis, can produce flat-topped transverse intensity profiles—as observed. We may therefore have evidence that the internal jet structure postulated by Laing also occurs in this moderately-powered FR II source.

Acknowledgments. We thank Harvey Liszt for his DRAWSPEC 1D-profile reduction package, the AIPS group for their VLA imaging software, and our colleagues at the NRAO for forbearance while our data were being processed. MRS thanks the workshop organizers for financial support. The National Radio Astronomy Observatory is a facility of the National Science Foundation, operated under a cooperative agreement by Associated Universities, Inc.

References

Clarke, D. A., Bridle, A. H., Burns, J. O., Perley, R. A., & Norman, M. L. 1992. "Origin of the structures and polarization in the classical double 3C 219", *ApJ*, **385**, 173–187.

Katz-Stone, D. M., & Rudnick, L. 1994. "Isolating the physical parameters of synchrotron sources", *ApJ*, **426**, 116–122.

Laing, R. A. 1993. "Radio observations of jets: large scales", in *Space Telescope Sci. Inst. Symp. 6: Astrophysical Jets*, eds. D. Burgarella, M. Livio, & C. O'Dea (Cambridge: Cambridge Univ. Press), 95–119.